MESOSCALE SIMULATION OF ATMOSPHERIC RESPONSE TO CHAOS TERRAIN FORMATION.
E.S. Kite[1], S.C.R. Rafkin[2], T.I. Michaels[2], M. Manga[1]. [1]Earth and Planetary Science, University of California, Berkeley (kite@berkeley.edu), [2] Department of Space Studies, Southwest Research Institute, Boulder, Colorado.

Introduction: Water ponded within Juventae and Echus Chasmata during outflow channel formation [1]. Unusually young channel networks are preserved on plateaux to the W of both chasms [2-3], superimposed on Late Hesperian basalts. The Juventae Chasma plateau channel networks are preserved in inverted relief, within light-toned layered deposits that contain opal and hydroxylated ferric sulfate [4-5]. Cross-cutting relationships imply that channel formation was episodic, beginning before backwasting of the chasm walls to their present position, but continuing afterwards [6]. Localized precipitation during chaos terrain formation has been proposed to explain these channels [7]. We report preliminary results from MRAMS (Mars Regional Atmospheric Modeling System) mesoscale simulations intended to test this hypothesis. These preliminary results are consistent with the localized-precipitation hypothesis, and suggest that storms associated with chaos terrain formation may mobilize sand and perhaps gravel, but not boulders.

Model description: MRAMS is a regional mesoscale model of the Martian atmosphere with non-hydrostatic, fully compressible dynamics and dust, water ice, and CO_2 ice aerosol microphysics [8-9]. Liquid water aerosol is not included. In the runs reported here, we used 4 nested grids with the innermost grid having a horizontal resolution of 8.33 km, and a vertical resolution of 30 m at the surface. Surface layer fluxes of heat, momentum and moisture are parameterized using a Monin-Obukhov scheme.

Boundary conditions: We flooded Juventae Chasma to -1000m, fixing lake surface temperature to 278.15K. In these preliminary runs, lake surface roughness was unchanged from the land value (z_0 = 0.03m). Boundary conditions for MRAMS are from "normal year" output from the NASA Ames GCM at $L_s \sim 270°$. To prevent lake surface saturation vapor pressures greater than atmospheric pressure, we doubled atmospheric pressure throughout the simulation. Gullies at high elevations suggest that atmospheric pressure was modestly greater in the geologically recent past [10]. Following a spin-up period without vapor release from the lake, the model was run for an additional 1.25 days with vapor release from the lake. After a brief (< ½ day) adjustment period, the location and rate of water-ice precipitation stabilized, although there is some variation with time-of-day. Once water-ice reaches the ground, albedo is set to 0.7.

Model output: Condensation of vapor released by the lake drives a circulation in the vertical plane with some similarities to tropical cyclones on Earth: strong low-level winds converge in the south of the lake, leading to high water vapor mass fractions (up to 0.3) near the surface. Maximum water ice mass fractions (~1%) and vertical velocities (~50 m/s) occur ~30 km above the lake surface.

Water-ice precipitation on the chasm flanks has two local maxima: on a promontory northwest of Juventae Chasma, and near the center of the south wall of Juventae Chasma. There is good spatial correspondence (Figure 1) between the first local maximum and the inverted channels and light-toned layered deposits mapped with HiRISE [6]. However, there is no evidence for channels or light-toned layered deposits in available (CTX) images of the south chasm wall. We find high precipitation rates are restricted to the immediate vicinity of the lake. Excluding snowfall back into the lake (60% of total snow), 50% of the snow falls within 75 km of the lake edge, and 95% within 200 km. The mapped layered deposits and inverted channels [6] fall within 50 km of the lake edge.

Sensitivity tests show a trend of reduced vapor release with reduced grid spacing in z, so the modeled precipitation rates are probably overestimated. On the plateau, this rate peaks at ~3 g/cm^2/day.

Energy and water budgets: Net evaporation from the lake (0.9 g/m^2/s) is approximately equal to the accumulation rate of water ice beyond the lake margins. Assuming a mixing depth of 100m, this corresponds to evaporative cooling of ~0.5 K / day. To prevent freezing of the lake surface, either energy must be delivered from deeper parts of the lake (by wind-driven mixing or convection), or warm, buoyant water must be continuously supplied from fractures at the lake floor. Existing models of chaos hydrology [1, 11] show discharge rates that exceed our simulated evaporation rates for hours to months, depending on assumed aquifer permeability. The temperature of the released water will evolve during the chaos event and will depend on the aquifer depth, the geothermal gradient, and the presence/absence of a triggering volcanic intrusion [12]. Alternatively, stresses during spillway breaching and outflow channel formation could mechanically disrupt ice cover.

Comparison with observed channels and layered deposits: We traced all inverted channels in HiRISE image PSP_003724_1755, obtaining a drainage density of 1.33 km^{-1}. Following the method of [13], we calcu-

late the necessary melt rate to initiate sediment transport as a function of friction factor and grain size (Figure 2). Mobilization of clasts greater than 1 HiRISE pixel in diameter requires melting rates much greater than the simulated precipitation rates. To date no HiRISE-resolvable clasts have been reported: any future detections would be a severe challenge to the localized-precipitation hypothesis.

MRAMS tracks the accumulation of dust as ice particle nuclei. Assuming silicate dust density, the dust accumulation rate is < 1 cm/yr. Observed light-toned layer thicknesses are ~1 m [6], so if each layer corresponds to one chaos event < 1 yr in duration, an additional source of silicates is needed. That source could be pre-existing aeolian deposits unrelated to the chaos event, or volcanic ash.

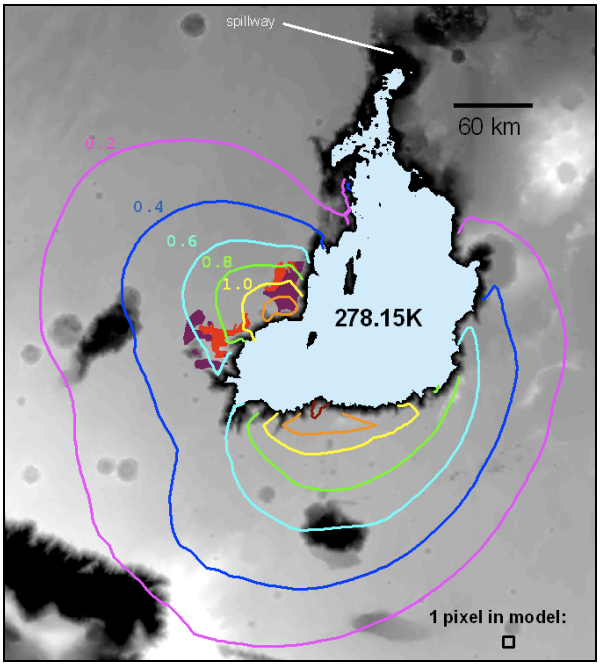

Figure 1. Water-ice precipitation rate (mm/hr), overlain on MOLA topography (white is high, black is low, elevation ranges from +5 to -3 km). Pale blue shade corresponds to Juventae Chasma flooded to -1000 m with water at 5°C. Contours at 0.2 mm/hr intervals. Red and purple shades northwest of the chasm correspond to inverted channels and light-toned layered deposits, respectively [6].

Next steps: Desirable improvements include a dynamic lake surface roughness parameterization [15] and self-consistent lake thermodynamics. At the moment, MRAMS treats water vapor as a trace gas (the pressure and virtual temperature effects of vapor release are not included). Other channels/layered deposits on the Valles Marineris plateau close to chaos terrains include Ganges Chasma and Echus Chasma: these are future modeling targets.

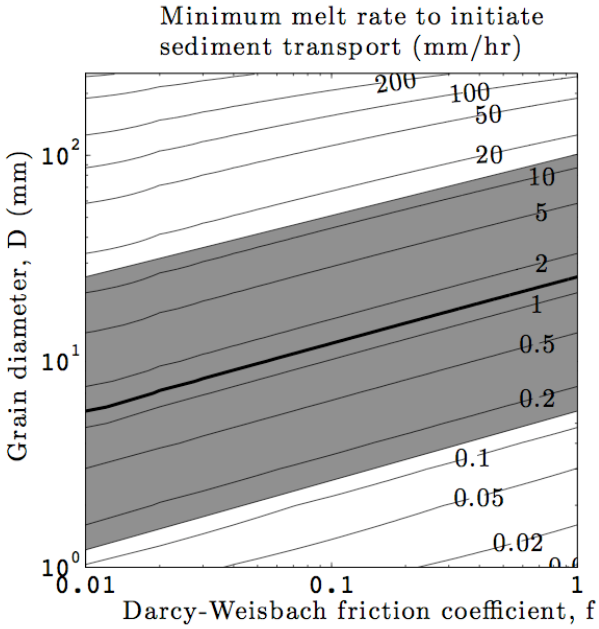

Figure 2. Minimum melting rate (mm/hr) to initiate sediment transport (calculated using equation 6 in [13]), for a single inverted channel in HiRISE image PSP_003724_1755. Parameters (how obtained) are S = 0.44° (MOLA), W = 8 – 11.25 m (HiRISE), A = 2.6 km^2 (HiRISE), g = 3.7 ms^{-2}, τ^*_c = 0.05, and ρ' = 2. The simulated peak precipitation rate is 1.3 mm/hr (thick solid line), although this may be an overestimate (see text). The gray band represents order-of-magnitude uncertainty in peak precipitation rate. Melt rates can exceed precipitation rates if seasonal cycles act as a capacitor.

References: [1] Harrison K.P. & Grimm R.E. (2008) *JGR,* 113, doi:10.1029/2007JE002951. [2] Mangold, N., et al. (2004) *Science*, 305, 78-81. [3] Williams, R.M.E., et al (2005), *LPSC XXXVI*, Abstract #1173. [4] Milliken, R.E., et al. (2008) *Geology*, 36, 847-850. [5] Bishop, J.L., et al. (2009) *JGR*, 114 doi:10.1029/ 2009JE003352, [6] Weitz, C.M., et al. *Icarus,* in press. [7] Mangold, N., et al. (2008) *JGR*, 113, doi:10.1029/2007JE002985. [8] Rafkin, S.C.R., et al. (2001) *Icarus*, 151, 2282-256. [9] Michaels, T.I., & Rafkin, S.C.R. (2008) *3rd Int'l Workshop on The Mars Atmosphere*, Abstract #9116. [10] Head, J.W., et al. (2008), *PNAS*, 105, 13258-13263. [11] Andrews-Hanna, J.C., & Phillips, R.J. (2007) *JGR*, 112, doi:10.1029/2006JE002881. [12] McKenzie, D. & Nimmo F. (1999) *Nature*, 397, 231-233. [13] Perron, J.T., et al. (2006) *JGR*, 111, doi:10.1029/ 2005JE002602. [14] Hecht, M.H. (2002) *Icarus*, 156, 373-386. [15] § 7.2 in Pielke Sr., R.A. (2002) Mesoscale meteorological modeling, 2nd edn.